



Study on the microstructure and performance of laser cladding-rolling compaction hybrid forming for 15-5PH stainless steel

Mengyuan Wu¹, Minghui Cai^{1,a,†}, Jixin Yang^{2,b}, Xiaoqi Hu² and Yunjie Bi²

¹*School of Materials Science and Engineering, Northeastern University, Shenyang 110819, China*

²*Institute of Advanced Additive Manufacturing, Ji Hua Laboratory, Foshan, China*

E-mail: ^{a,†}caimh@smm.neu.edu.cn, ^byangjx@jihualab.ac.cn

15-5PH samples were prepared using the laser cladding-rolling compaction hybrid forming process, and the impact mechanism of rolling force on the microstructure and properties of the samples during the composite forming process was systematically studied. The results indicate that under the laser cladding-rolling compaction hybrid forming process, the martensite laths are refined, and in addition to columnar grains parallel to the deposition direction, some martensite laths undergo a change in orientation, approaching parallel to the printing plane direction. The improvement in the characteristics of the microstructure caused by the laser cladding-rolling compaction hybrid forming process further leads to enhancement of surface hardness of the components.

Keywords: Laser Cladding-rolling; Compaction Hybrid Forming; 15-5PH; Microstructure.

1. Introduction

Laser cladding technology uses lasers as the heat source, depositing material layer by layer according to a computer-generated path to create three-dimensional geometric parts [1]. This technology is widely used in aerospace, automotive, and aircraft engine industries due to its high processing flexibility, short production cycles, and ease of digital control. During laser cladding, the high-energy heat source and rapid movement of the small molten pool result in a very high temperature gradient and rapid cooling rate [2, 3], causing the solidified structure to grow along the direction of deposition. When the molten pool interacts with complex fluid dynamics during melting and solidification, gases can become trapped, or unmelted powder may remain, leading to the frequent occurrence of pores and cracks in the formed parts [3, 4]. These defects, and the directional growth of the solidification structure, adversely affect the performance of the components, thereby limiting the application and promotion of metal laser cladding manufactured parts [5].

The flexibility of laser cladding in the forming process allows it to be combined with auxiliary technologies such as electromagnetic fields, mechanical vibrations, micro-arcs, and laser impacts, thus reducing defects and improving forming efficiency. For example, Y Wang and others [6] have used a hybrid process consisting of laser cladding and in-situ ultrasonic shot peening to prepare Inconel 718 superalloy samples. The results show that this hybrid additive manufacturing process can produce high-quality metal parts with

[†] This work is supported by grant 51975111 of the National Natural Science Foundation and grant X190351TM190 of the Ji Hua Laboratory.

significantly refined microstructures and beneficial residual compressive stresses along the surface depth. W Chen and others [7] have used a process combining layer-by-layer ultrasonic rolling treatment with laser cladding to prepare 15-5PH steel, showing that the process produces higher surface compressive stresses, reduces oxide inclusions, and refines martensite blocks. S Y Fan and others [8] have studied the macroscopic morphology, microstructure, and molten pool flow behavior of 316 stainless steel cladding layers under a high-frequency pulse-laser cladding composite process, demonstrating that under the effect of high-frequency pulse lasers, grain size is significantly refined due to increased nucleation tendency and reduced temperature gradient.

Given the limited research on laser cladding-rolling compaction composite manufacturing, the impact mechanisms on the formed structure and properties are not yet clear. Based on this, this paper uses laser cladding-rolling compaction composite manufacturing equipment to prepare single-pass single-layer and single-pass multi-layer 15-5PH stainless steel samples to study the effects of different rolling forces on the microstructure and properties of the alloy.

2. Experimental procedures

2.1. Materials and equipment

The experiment used gas-atomized 15-5PH stainless steel powder and a self-developed laser cladding-rolling compaction hybrid equipment, as shown in fig 1. To study the impact of roll pressure on the microstructure and properties of the hybrid-formed parts, single-pass single-layer and single-pass multi-layer samples were formed under various rolling forces, as shown in fig 2.

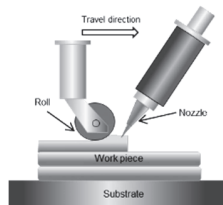


Fig. 1. Schematic Diagram of Laser Cladding-rolling Compaction Composite Forming.

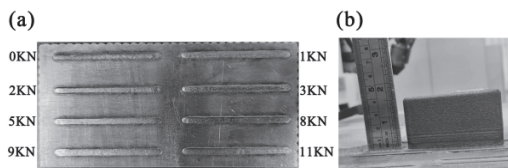


Fig. 2. (a) Single pass single layer sample of laser cladding-rolling compaction composite forming; (b) Single pass multi-layer sample of laser cladding-rolling compaction composite forming.

2.2. Materials characterization

After Manufacturing is Completed, the samples were prepared for microstructure characterization and tensile testing using electrical discharge machining wire cutting. Post-

formation, the samples were ground sequentially using sandpaper from 400 to 2000 grit, then polished to a scratch-free mirror finish. The samples were then etched in a solution of 4% HF + 4% HNO₃ + 92% H₂O for about 10 seconds until they turned a pale yellow color, followed by rinsing with water and cleaning with alcohol. Microstructural observations were carried out using an optical microscope and a Scanning Electron Microscope (SEM) and microhardness tests were performed using a micro Vickers hardness tester. The grain morphology at different locations was characterized using electron backscattered diffraction (EBSD). The EBSD samples were electro-polished at room temperature using a solution containing 5% perchloric acid and 95% acetic acid. The EBSD scans were performed at a voltage of 20 KV with a step size of 0.5 μ m.

3. Results and discussion

The cross-sectional microstructure of the single-pass 15-5PH stainless steel samples formed by laser cladding-rolling compaction under different rolling forces is shown in Figure 3. During the rolling process, mechanical energy is converted to thermal energy, which slows down the cooling rate of the melt pool and enhances its spreadability, resulting in a reduction in the height of the deposited layer and its expansion to the sides^[9]. With the increase in rolling force, the height of the sample decreases while the width of the vertical cross-section increases.

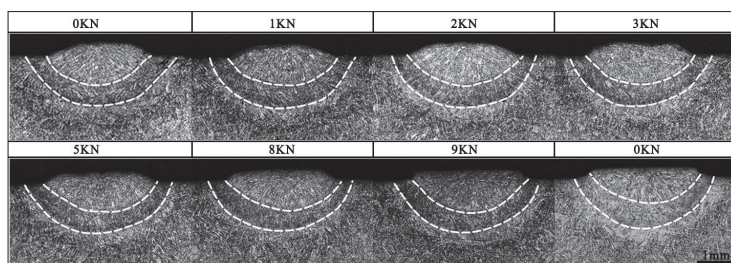


Fig. 3. Morphology of the melt pool for the single pass single layer sample of 15-5PH using laser cladding-rolling compaction composite forming.

Fig 4 shows the SEM image of a single-pass multi-layer 15-5PH steel along the deposition direction in laser cladding-rolling composite forming. It can be seen that the microstructure mainly consists of columnar martensite when no rolling force is applied. Upon the application of rolling force, the martensite undergoes deformation, and this phenomenon becomes more pronounced with the increase of rolling force.

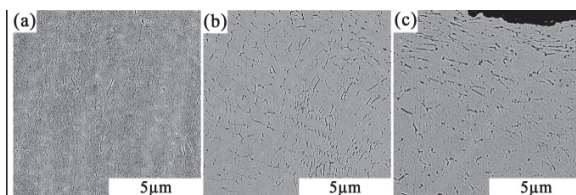


Fig. 4. SEM Image of a Single-Pass Multi-Layer Sample of 15-5PH Stainless Steel along the Deposition Direction in Laser Cladding-Rolling Composite Forming.

Fig 5 shows the EBSD results from the top and bottom along the deposition direction. From Fig 5(a) and 5(d), it can be seen that due to the characteristics of rapid solidification and cooling during the forming process, the microstructure of the laser-clad 15-5PH stainless steel consists of columnar martensite perpendicular to the substrate^[10]. Fig 5(b) and 5(e) reveal that under a pressure of 5 kN, the microstructure of the composite-formed sample is finer. Besides the columnar crystals perpendicular to the base plate, the orientation of some martensite laths changes to become more parallel to the horizontal direction, and this phenomenon is more pronounced at 10 kN.

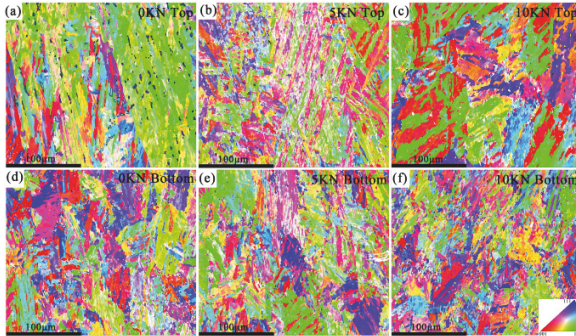


Fig. 5. EBSD orientation map of the multi-layer single pass sample of 15-5PH stainless steel along the deposition direction using laser cladding-rolling compaction composite forming.

Fig 6 presents the hardness distribution along the deposition direction. Due to the cooling of the bottom microstructure through the cold base plate, the martensitic transformation occurs at a higher cooling rate^[11]. The phase transformation strengthening, solid solution strengthening, and fine grain strengthening of the martensitic structure result in higher hardness at the bottom of all samples, around 430 HV. As the cladding layers increase, the hardness decreases to approximately 350 HV due to the accumulation of heat and the remelting effect of the cladding layer on the previous layer, gradually stabilizing. Under rolling pressures of 0 kN, 5 kN, and 10 kN, the average Vickers hardness of the samples is 356 HV, 359 HV, and 377 HV, respectively. As shown in Figure 5, with the increase in rolling force, the grains are refined, which results in an increase in the hardness of the samples.

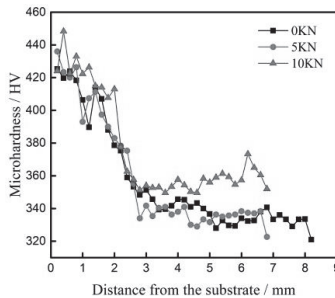


Fig. 6. Vickers hardness along the deposition direction of the multi-layer single pass sample of 15-5PH stainless steel in laser cladding-rolling compaction composite forming.

4. Conclusions

(1) The quality of the 15-5PH stainless steel formed by laser cladding-rolling compaction composite forming is good and coherent. As the rolling force increases, the height of the sample decreases, and the width of the vertical cross-section increases.

(2) As the rolling force increases, some of the martensitic laths tend to orient and grow parallel to the horizontal direction, and the martensitic structure is refined.

(3) As the rolling force increases, the hardness of the composite formed 15-5PH steel increases

References

1. S. J. Xu, C. Y. Quan. Current Status and Future Prospects of Metal Additive Manufacturing Technology in the Aerospace Industry, *J. Powder Metallurgy Industry*. **32**, 9 (2022).
2. W. King, A. Anderson. Applied Physics Reviews, *J.* (2015).
3. Q. Guo, C. Zhao. In-situ characterization and quantification of melt pool variation under constant input energy density in laser powder bed fusion additive manufacturing process, *J. Additive Manufacturing*. **28**, 600 (2019).
4. P. S. Cook, A. B. Murphy. Simulation of melt pool behaviour during additive manufacturing: Underlying physics and progress, *J. Additive Manufacturing*. **31**, 100909 (2020).
5. Z. Liu, D. Zhao. Additive manufacturing of metals: Microstructure evolution and multistage control, *J. Journal of Materials Science Technology*. **100**, 224 (2022).
6. Y. Wang, J. J. M. Shi, M. T. B. Microstructure and properties of Inconel 718 fabricated by directed energy deposition with in-situ ultrasonic impact peening, *J.* **50**, 2815 (2019).
7. W. Chen, L. Xu. Application of hybrid additive manufacturing technology for performance improvement of martensitic stainless steel, *J. Additive Manufacturing*. **51**, 102648 (2022).
8. S.Y.Fan, J.Z.Mao. The Effect of Pulsed/Continuous Dual Beam Composite Laser Cladding on the Microstructure of 316L Stainless Steel Claddings, *J. Chinese Journal of Lasers*. **50**, 11 (2023).
9. J. Yang, Y. Chen. Hierarchical microstructure of a titanium alloy fabricated by electron beam selective melting, *J. Journal of Materials Science Technology*. **42**, 1 (2020).
10. H. H. Bajguirani. The effect of ageing upon the microstructure and mechanical properties of type 15-5 PH stainless steel, *J. Materials Science Engineering: A*. **338**, 142 (2002).
11. L. Couturier, F. De Geuser, M. Descoins. Evolution of the microstructure of a 15-5PH martensitic stainless steel during precipitation hardening heat treatment, *J. Materials and Design*. **107**, 416 (2016).

Open Access This chapter is licensed under the terms of the Creative Commons Attribution-NonCommercial 4.0 International License (<http://creativecommons.org/licenses/by-nc/4.0/>), which permits any noncommercial use, sharing, adaptation, distribution and reproduction in any medium or format, as long as you give appropriate credit to the original author(s) and the source, provide a link to the Creative Commons license and indicate if changes were made.

The images or other third party material in this chapter are included in the chapter's Creative Commons license, unless indicated otherwise in a credit line to the material. If material is not included in the chapter's Creative Commons license and your intended use is not permitted by statutory regulation or exceeds the permitted use, you will need to obtain permission directly from the copyright holder.

